Astron. Astrophys. 350, 970–984 (1999)

ASTRONOMY AND ASTROPHYSICS

The wind momentum-luminosity relationship of galactic A- and B-supergiants

R.P. Kudritzki[1,2,3], **J. Puls**[1], **D.J. Lennon**[1,4], **K.A. Venn**[5], **J. Reetz**[1], **F. Najarro**[9], **J.K. McCarthy**[6], **and A. Herrero**[7,8]

[1] Institut für Astronomie und Astrophysik der Universität München, Scheinerstrasse 1, 81679 München, Germany
[2] Max-Planck-Institut für Astrophysik, Karl-Schwarzschild-Strasse 1, 85740 Garching, Germany
[3] University of Arizona, Steward Observatory, 933 N. Cherry Av., Tucson, AZ 85721, USA
[4] Isaac Newton Group of Telescopes, Apartado de Correos 368, 38700 Santa Cruz de La Palma, Spain
[5] Department of Physics and Astronomy, Macalaster College, St.Paul, MN 55101, USA
[6] Palomar Observatory, California Institute of Technology, Pasadena, CA 91125, USA
[7] Instituto de Astrofísica de Canarias, c/Vía Lactea s/n, 38200 La Laguna, Tenerife, Spain
[8] Departamento de Astrofisica, Universidad de La Laguna, Avda. Astrof. Francisco Sanchez s/n, 38071 La Laguna, Spain
[9] Instituto de Estructura de la Materia, CSIC, Serrano 121, 28006 Madrid, Spain

Received 28 April 1999 / Accepted 27 August 1999

Abstract. The Balmer lines of four A Ia-supergiants (spectral type A0 to A3) and fourteen B Ia and Ib-supergiants (spectral type B0 to B3) in the solar neighbourhood are analyzed by means of NLTE unified model atmospheres to determine the properties of their stellar winds, in particular their wind momenta. As in previous work for O-stars (Puls et al. 1996) a tight relationship between stellar wind momentum and luminosity ("WLR") is found. However, the WLR varies as function of spectral type. Wind momenta are strongest for O-supergiants, then decrease from early B (B0 and B1) to mid B (B1.5 to B3) spectral types and become stronger again for A-supergiants. The slope of the WLR appears to be steeper for A- and mid B-supergiants than for O-supergiants. The spectral type dependence is interpreted as an effect of ionization changing the effective number and the line strength distribution function of spectral lines absorbing photon momentum around the stellar flux maximum. This interpretation needs to be confirmed by theoretical calculations for radiation driven winds.

The "Pistol-Star" in the Galactic Centre, an extreme mid B-hypergiant recently identified as one of the most luminous stars (Figer et al. 1998) is found to coincide with the extrapolation of the mid B-supergiant WLR towards higher luminosities. However, the wind momentum of the Luminous Blue Variable P Cygni, a mid B-supergiant with extremely strong mass-loss, is 1.2 dex higher than the WLR of the "normal" supergiants. This significant difference is explained in terms of the well-known stellar wind bi-stability of supergiants very close to the Eddinton-limit in this particular range of effective temperatures. A-supergiants in M31 observed with HIRES at the Keck telescope have wind momenta compatible with their galactic counterparts.

The potential of the WLR as a new, independent extragalactic distance indicator is discussed. It is concluded that with ten to twenty objects, photometry with HST and medium resolution spectroscopy with 8m-telescopes from the ground distance moduli can be obtained with an accuracy of about $0\overset{\mathrm{m}}{.}1$ out to the Virgo and Fornax clusters of galaxies.

Key words: stars: atmospheres – stars: early-type – stars: mass-loss – galaxies: distances and redshifts – cosmology: distance scale

Send offprint requests to: R.P. Kudritzki
(kudritzki@usm.uni-muenchen.de)

1. Introduction

The theory of radiation driven winds (Castor et al. 1975, Pauldrach et al. 1986, Kudritzki et al. 1989) predicts a tight relationship between the total mechanical momentum flow $\dot{M}v_\infty$ contained in the stellar wind outflow and the luminosity L of the mass-losing star

$$\dot{M}v_\infty \propto R_*^{-1/2} L^{1/\alpha_{\rm eff}}. \quad (1)$$

In Eq. 1 $\dot{M}$ is the mass-loss rate, v_∞ the terminal velocity of the stellar wind, and R_* the stellar radius. $\alpha_{\rm eff}$ is a dimensionless number of the order of $2/3$ and represents the power law exponent of the distribution function of line strengths of the thousands of spectral lines driving the wind. (For a simplified derivation of Eq. 1, see Kudritzki 1998, or Kudritzki 1999a).

Analyzing H_α line profiles of O-stars in the Galaxy and in the Magellanic Clouds Puls et al. (1996) were able to demonstrate that such a relationship does indeed exist for the most luminous O-stars ranging over 1 dex in stellar luminosity. In addition, Kudritzki et al. (1997) found that Central Stars of Planetary Nebulae being equally hot or hotter than O-stars but two orders of magnitudes less luminous show wind momenta corresponding to the relationship for O-stars extrapolated towards lower luminosities.

The existence of such a relationship introduces a variety of new and interesting aspects. First of all, if reliably calibrated,

it can be used to determine distances by purely spectroscopic means with mass-loss rates and terminal velocities obtained directly from line profiles yielding absolute stellar luminosities. Second, together with the well known proportionality of v_∞ to the escape velocity v_{esc} from the stellar surface (Abbott 1982) it provides a simple way to predict stellar wind energy and momentum input into the interstellar medium from clusters and associations of hot stars. Third, it may be used to estimate mass-loss rates, wind energies and momentum along sequences of stellar evolutionary tracks (for a more detailed discussion of these aspects, see Kudritzki 1999a).

With this in mind, we have started to investigate whether the winds of luminous blue supergiants of spectral types later than O also follow a relationship as described by Eq. 1. From the viewpoint of theory this is clearly to be expected, although it is very likely that the proportionality constant and the exponent $\alpha_{\rm eff}$ will be different, since the winds of A- and B-supergiants are driven by lines of different ionization stages. However, our hope is that a similarily tight relationship may exist. This would allow to extend the simple description of stellar wind strengths towards later stages of stellar evolution. Even more important, it would render the possibility to use the optically brightest "normal" stars, super- and hypergiants of spectral type A and B, as new primary extragalactic distances indicators for galaxies far beyond the Local Group. In a first pragmatic step, Kudritzki et al. (1995) used mass-loss rates obtained by Barlow & Cohen (1977) from IR-photometry and first estimates of terminal velocities to find indeed an indication for such a relationship at later spectral types.

In this paper, we present the first results of our spectroscopic attempt to establish the Wind momentum – Luminosity Relationship (WLR) of galactic supergiants of spectral type A and B. We concentrate on a small number of objects with reasonably well determined distances. Optical spectra are used to obtain the stellar parameters of $T_{\rm eff}, \log g, R_*, L$. Then, H_α-line profiles are analyzed in detail to determine the stellar wind properties, in particular the mass-loss rates. Together with terminal velocities measured from from UV-resonance lines and H_α (for A-supergiants) this yields stellar wind momenta as function of the stellar luminosities.

2. Model atmospheres for the stellar wind analysis

The determination of stellar wind parameters from the Balmer lines of blue supergiants requires the sophisticated effort of using NLTE unified model atmospheres with stellar winds and spherical extension, as originally introduced by Gabler et al. (1989). These new types of model atmospheres provide a smooth transition from the subsonic, quasi-hydrostatic photosphere to the supersonic stellar wind and allow to deal simultaneously with wind contaminated absorption lines like H_γ and pronounced stellar wind emission lines such as H_α. They are also essential for stars with weak winds, when H_α turns into an almost photospheric absorption line, a situation impossible to deal with quantitatively by treating photosphere and wind as separated entities. For our work, we use the new unified model code developed recently by Santolaya-Rey et al. (1997, hereafter SPH). This new code is extremely fast and produces a unified model in few minutes on a work station, which is crucial for a project aiming at the analysis of many stars with different stellar parameters and different wind properties. In addition, it has the advantage of being numerically stable over the entire domain of O-, B- and A-stars in the HRD, independent of the adopted stellar wind strengths. The code can deal with extreme emission lines produced by very strong winds as well as with an entire absorption spectrum for extremely weak winds. In these latter cases it re-produces perfectly the line profile results of plane-parallel, hydrostatic NLTE model atmosphere codes. As SPH have shown, this is only possible because the Sobolev approximation is avoided and the NLTE multilevel radiative transfer is treated in the comoving frame of the stellar wind outflow velocity field. In addition, incoherent electron scattering can be included in the final formal integral to calculate the line profiles. This is important for low gravity A-supergiants, where *photospheric* electron-scattering produces shallow and wide emission wings (see SPH and McCarthy et al. 1997).

A unified model atmosphere is defined by the effective temperature $T_{\rm eff}$, the gravity $\log g$ and the stellar radius R_* at the Rosseland optical depth $\tau_{\rm ross} = 2/3$ together with $\dot{M}$, v_∞ and the parameter β which describes the radial slope of the velocity field via

$$v(r) = v_\infty (1 - b/r)^\beta. \qquad (2)$$

The constant b is chosen to guarantee a smooth transition into the hydrostatic stratification at a prespecified outflow velocity smaller than the isothermal sound speed (normally 0.1 $v_{\rm sound}$). Observed velocity fields are usually well represented by this parametrization.

As for the analysis of O-star stellar wind lines in the UV (see Haser et al. 1998 for a most recent reference) the assumption of a local Gaussian microturbulent velocity $v_{\rm t}$ is needed to fit the wind affected Balmer line profiles of B- and A-supergiants. For simplicity, we adopt a constant value of $v_{\rm t}$ through the entire atmosphere. We are aware of the fact that a stratified turbulent velocity field increasing outwards (as for O-stars, see Haser et al. 1998) would probably be more appropriate. However, since the determination of wind momenta is only little affected by any assumption concerning the microturbulence, we postpone the inclusion of depth dependent microturbulence to a later study. In some cases we find that the fit of H_γ requires a smaller value of $v_{\rm t}$ than H_α. We attribute this to a stratification of the microturbulent velocity.

The spectral lines of B- and A- supergiants are also broadened by stellar rotation. We determined rotational velocities $v_{\rm rot}$ from weak metal lines in the optical spectra by a comparison of observed line profiles with computations assuming an intrinsically narrow (only thermally broadened) line which was convolved with a rotational and instrumental broadening function. For the B-supergiants we compared these results with the values obtained by Howarth et al. (1997) from IUE high resolution spectra. In most cases our $v_{\rm rot}$ values were somewhat smaller corresponding to a systematically difference of 12 percent. We

Table 1. Adopted distance moduli

assoc.	m-M	source
Per OB1	$11\overset{m}{.}8$	Garmany & Stencel, 1992
Ori OB1	$8\overset{m}{.}5$	Blaha & Humphreys, 1989
Gem OB1	$10\overset{m}{.}9$	Blaha & Humphreys, 1989
Cyg OB1	$10\overset{m}{.}5$	Garmany & Stencel, 1992
Cas OB5	$11\overset{m}{.}5$	Garmany & Stencel, 1992
Cas OB14	$10\overset{m}{.}2$	Blaha & Humphreys, 1989
Car OB1	$12\overset{m}{.}5$	see text, Sect. 6
Col 121	$9\overset{m}{.}2$	Blaha & Humphreys, 1989
Cep OB2	$9\overset{m}{.}9$	Garmany & Stencel, 1992

Table 2. Spectral types and photometric data of B-supergiants

star	spec. type	assoc.	m_v	B-V	E(B-V)	M_v
HD			mag	mag	mag	mag
37128	B0Ia	Ori OB1	1.70	-0.19	0.06	-6.99
38771	B0.5Ia	see text	2.04	-0.18	0.06	-4.80
2905	BC0.7Ia	Cas OB14	4.16	0.14	0.31	-7.00
13854	B1Iab	Per OB1	6.47	0.28	0.50	-6.70
13841	B1.5Ib	Per OB1	7.36	0.23	0.41	-5.57
193183	B1.5Ib	Cyg OB1	7.00	0.44	0.64	-5.47
41117	B2Ia	Gem OB1	4.63	0.27	0.42	-7.54
14818	B2Ia	Per OB1	6.25	0.30	0.48	-6.87
14143	B2Ia	Per OB1	6.64	0.50	0.65	-6.95
206165	B2Ib	Cep OB2	4.74	0.30	0.48	-6.40
13866	B2Ib	Per OB1	7.49	0.19	0.37	-5.33
42087	B2.5Ib	Gem OB1	5.75	0.22	0.38	-6.32
53138	B3Ia	Col 121	3.01	-0.11	0.06	-6.37
14134	B3Ia	Per OB1	6.57	0.48	0.69	-7.13

attribute this to the different technique applied but note that for the determination of wind momenta this small difference is not important.

3. Spectroscopic data

Blue and red spectra were available for all of our targets. The B-supergiant data have been obtained by DJL and are described in Lennon et al. (1992, 1993) and McErlean et al. (1999). For the A-supergiants (except HD 92207) the spectra were taken by KAV using the Coude-spectrograph at the 2.1m-telescope at McDonald Observatory, Texas (see Venn 1995a,b for a more detailed description of the setup used). For HD92207 Echelle-spectra obtained with the ESO 50 cm-telescope at La Silla (see Kaufer et al. 1996) were provided by A. Kaufer (LSW Heidelberg). For the analysis presented below it is important to note that the S/N of all spectra used is better than 100 and that the spectral resolution at H_α exceeds the photospheric rotational velocities.

4. Distances

To calibrate the WLR the stellar radii and, therefore, the distances must be known. For A- and B-supergiants this is a major source of uncertainty, since most of these objects in the solar neighbourhood are already to remote too allow a direct measurement of parallaxes. Therefore, distances have to be determined from association and cluster membership. For our work we have selected objects belonging to Per OB1, Ori OB1, Gem OB1, Cyg OB1, Cas OB5, Cas OB14, Car OB1, Cep OB2and Col 121 (see Table 1).

One object, HD 38771 (κ Ori) appears to be in the foreground of its association according to the Hipparcos-catalogue, which gives $\pi = 4.52$ and $\sigma = 0.77$ (in μarcsec) for parallax and standard deviation, respectively. Although also quite uncertain in view of the recent discussion of Hipparcos data (see Narayanan & Gould 1999; Reid 1998) and hard to believe in view of the average absolute magnitude of early B Ia supergiants, we make use of this distance.

5. Spectral analysis of B-supergiants

14 B-supergiants of luminosity class I and spectral types B0 to B3 have been selected from the list of objects studied by Lennon et al. (1992, 1993) according to the criteria that reasonable measurements of v_∞ from ultraviolet spectra and estimates of the distance modulus are available. For normal B-supergiants of spectral types later than B3 it is difficult to determine v_∞ from the UV (see Howarth et al. 1997). This explains why we have not included spectral types B4 to B9 in this study, although H_α profiles indicate the significant presence of winds in many cases.

The photometric data (from Blaha & Humphreys 1989), association or cluster membership and spectral type (from the compilation by Howarth et al. 1997, see references therein) are given in Table 2. To calculate the de-reddened absolute magnitude M_v a value of R_v=3.1 has been adopted for the ratio of interstellar extinction A_v to reddening E(B-V) for all objects except those in Per OB1 (R_v=2.75) and Cep OB2 (R_v=2.6). These latter values have been proposed by Cardelli et al. (1989).

5.1. Stellar parameters

The stellar parameters are obtained from the quantitative analysis of the spectrum. We adopt the effective temperatures determined in the NLTE analysis by McErlean et al. (1999) using unblanketed hydrostatic model atmospheres. Their $T_{\rm eff}$ scale is based on the He II/I ionization equilibrium for $T_{\rm eff} \geq$ 26000 K and on the Si IV/III ionization equilibria for the cooler B-supergiants in our sample. Then, we calculate unified model atmosphere fluxes for the V-filter to obtain stellar radii from M_v as described by Kudritzki (1980). Since unified model atmospheres are spherically extended, the predicted flux depends in principle also on the radius adopted for the model atmosphere calculations. This requires an iteration with regard to the stellar radius. However, as long as the mass-loss rates are not extremely large, the radius dependence of the model atmosphere flux is very weak so that the iteration is not necessary or converges very quickly, if needed. No attempts are made to re-determine effective temperatures using unified model atmosphere calculations of He I/He II or Si III/iv lines. This is possible, in principle, with our present version of the SPH-code

Table 3. Stellar parameters and stellar wind properties of B-supergiants

star	$T_{\rm eff}$	R_*	$\log g$	$\log L/L_\odot$	$v_{\rm rot}$	$v_{\rm t}$	β	v_∞	$\dot{M}$	$\log D_{\rm mom}$
HD	kK	$R_\odot$	cgs		km s^{-1}	km s^{-1}		km s^{-1}	10^{-6} $M_\odot$/yr	cgs
37128	28.5	35.0	3.00	5.86	80	20	1.25	1600.	2.40	29.15
38771	27.5	13.0	3.00	4.94	80	10	1.00	1350.	0.27	27.93
2905	24.0	41.0	2.70	5.70	60	20	1.35	1100.	2.30	29.01
13854	23.5	35.3	2.70	5.53	80	20	1.50	1000.	0.78	28.46
13841	22.0	22.9	2.70	5.04	75	20	3.0	1015.	0.038	27.06
193183	22.5	21.4	2.70	5.02	70	20	3.0	545.	0.035	26.74
41117	19.5	61.7	2.25	5.70	40	20	1.0	500.	0.85	28.32
14818	20.0	45.4	2.40	5.47	70	40	2.0	650.	0.25	27.83
14143	20.0	47.1	2.30	5.51	65	10	1.75	650.	0.30	27.92
206165	20.0	36.5	2.50	5.28	80	25	2.5	700.	0.060	27.20
13866	20.5	22.3	2.60	4.90	85	15	2.0	870.	0.020	26.71
42087	20.5	35.2	2.50	5.30	60	40	3.0	735.	0.11	27.48
53138	18.5	39.6	2.30	5.22	60	40	2.5	620.	0.095	27.37
14134	18.0	56.2	2.20	5.48	60	20	3.0	465.	0.15	27.52

but would increase the computational effort sigificantly for the large number of objects studied. Therefore, we postpone a completely self-consistent study iterating stellar parameters, chemical abundances and mass-loss rates at this stage.

In their NLTE study using hydrostatic, planeparallel model atmospheres McErlean et al. (1999) have also determined stellar gravities $\log g$ from a fit of the observed H_γ profiles. In our analysis, we start with their values but, since stellar wind emission as a function of the mass-loss rate does not only affect H_α but also higher Balmer lines such as H_β and H_γ (Gabler et al. 1989, Puls et al. 1996, Kudritzki 1998), we always checked the fits of these latter two Balmer lines and modified the gravity accordingly, if necessary. In most of the cases the $\log g$ values obtained by McErlean et al. (1999) were sufficiently accurate.

A normal helium abundance of N(He)/N(H)=0.1 was adopted for the calculation of all model atmospheres. The analysis of the observed He I spectra of B-supergiants still gives somewhat divergent results depending on the lines used for the abundance fit. However, the most recent investigations by McErlean et al. (1998, 1999) and Smith & Howarth (1998) indicate that helium enrichment is very likely to be small.

The stellar parameters obtained in this way are given in Table 3.

5.2. Stellar wind properties

In the determination of the stellar wind parameters from the Balmer lines we apply the same strategy as for O-stars (see Puls et al. 1996). We adopt terminal velocities v_∞ measured from radiative transfer fits of the strong UV resonance lines (Howarth et al. 1997, Haser 1995, see also Haser et al. 1995 and 1998). Then, we calculate unified models varying $\dot{M}, \beta$ and $v_{\rm t}$ to fit the Balmer lines. The strength of the stellar wind emission over the whole profile is a strong function of $\dot{M}$, whereas a variation of β affects only the central emission core and its halfwidth. In this way, it is possible to determine both quantities independently. $v_{\rm t}$ – as for the analysis of A-supergiants (see McCarthy et al. 1997) – influences the relative wavelength position of the H_α emission peak and weakly the width of H_γ absorption cores. For weak winds, where H_α is purely in absorption but partially filled in by wind emission, $v_{\rm t}$ has a crucial influence on the width of the H_α absorption core. We note that a careful adjustment of $v_{\rm t}$ helps to improve the general appearance of the line profile fit but has only little influence on the determination of the wind momentum.

The uncertainties of the stellar wind parameters obtained in this way depend on the strength of the stellar wind emission. For strong winds leading to a well pronounced wind emission in H_α, mass-loss rates can be determined with an accuracy of twenty percent. In the case of weak winds it is more difficult to constrain the value of β, which doubles the uncertainty of $\dot{M}$. Terminal velocities appear to be uncertain by fifteen percent. We estimate this number from a comparison of those objects in common between Howarth et al. (1997) and Haser (1995) (note in Table 3 we use the values given by Haser (1995), if available, and Howarth et al. (1997) otherwise). At the latest spectral type B3 this estimate might be a bit too optimistic, because of the weakness of wind features in the UV. (For instance, the v_∞ of HD 53138 measured by Haser (1995) is 40 percent smaller than the one determined by Howarth et al. (1997)). Generally, we expect wind momenta of objects with significant H_α emission to have an uncertainty of 0.1 dex and those of pure absorption line objects of 0.15 to 0.2 dex.

The results of the stellar wind analysis are summarized in Table 3. Profile fits of H_α and H_γ are given in Figs. 1, 2, 3, 4 and 5. The quality of the H_γ fits is remarkably good (note that the NLTE profile calculations did not include blends from the metal lines). In few cases, the values for $v_{\rm t}$ adopted for H_γ are smaller than those for H_α given in Table 3 (HD 193183 and 41117: 10 km s^{-1}, HD 206165 and 53138: 15 km s^{-1}, HD 14818 and 42087: 20 km s^{-1}). As already discussed above, we attribute this to a stratification of microturbulence through the wind. The smaller values for H_γ (as a more photospheric line) are in agree-

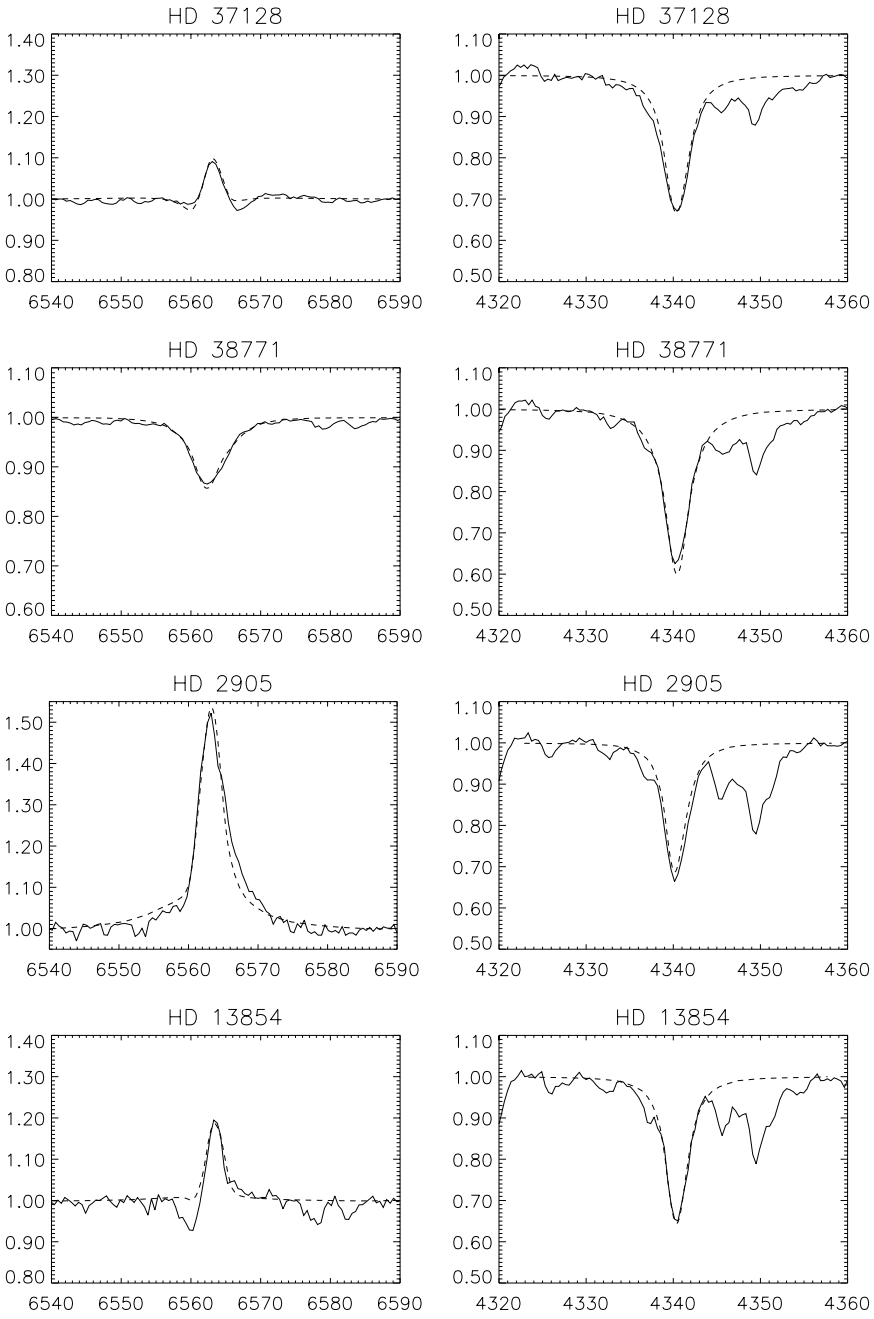

Fig. 1. H_α (left) and H_γ (right) line profile fits of the BIa-supergiants of spectral type B0 to B1.

ment with the results obtained by McErlean et al. (1999) in their study of photospheric metal and He I lines.

In view of the enormous variety of stellar wind strengths encountered, the H_α fits are also satisfactory. However, there are five objects (HD 13854, 41117, 14818, 14143, 14134), where the calculations fail to reproduce the observed absorption dip blueward of the emission peak. For two objects (HD 42087, 53138) with slightly weaker winds than those five the absorption dip is reproduced in its central depth but not in the width towards higher velocities. This might be the result of the neglect of metal line blanketing and blocking in our model atmospheres affecting the stratification of the NLTE H_α line source function through the expanding wind. We also note that we have neglected the influence of a possible He II blend at these rather low effective temperatures. Another explanation might be stellar wind variations and deviations from spherical symmetry and homogeneity leading to temporary absorption dips (see also the discussion in Puls et al. 1996, Kaufer et al. 1996, Kudritzki 1999b).

For three objects of our sample mass-loss rates have been determined from the continuous free-free stellar wind emission at radio wavelength by Scuderi et al. (1998). For HD 37128, HD 2905 and HD 41117 they obtained 2.1, 2.0 and 1.5 10^{-6} $M_\odot$/yr, in reasonable agreement with our H_α method. (Note that the distances adopted by Scuderi et al. are identical to ours, however their value of v_∞ for HD 37128 is somewhat higher. Using

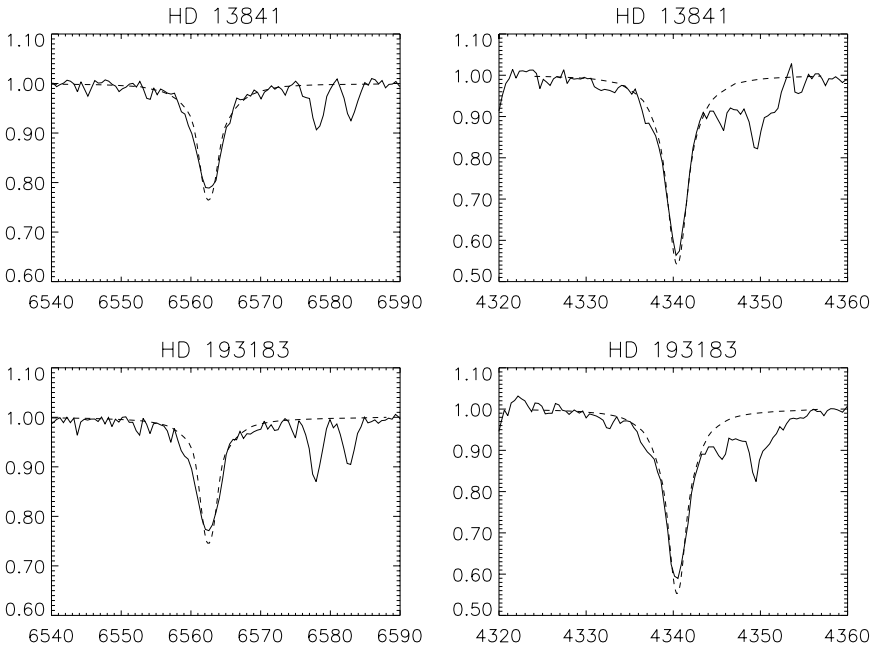

Fig. 2. H_α (left) and H_γ (right) line profile fits of the B 1.5 Ib supergiants.

our value and their observed radio fluxes we obtain 1.8 10^{-6} $M_\odot$/yr for the radio mass-los rate of HD 37128). For HD 53138 and HD 206165 upper limits of 4.0 and 6.0 10^{-7} $M_\odot$/yr for the mass-loss rate were determined by Drake & Linsky (1989) from radio flux measurements using the VLA. (We have scaled the Drake & Linsky results to our distances and values of v_∞). These limits may not be regarded as significant, as they are a factor of 4 and 10 higher than the mass-loss rates from our H_α determination. However, for HD 53138 Barlow & Cohen (1977) have measured a significant infrared excess at 10 micron requiring a factor 20 higher mass-loss rate than ours, if caused by free-free wind emission. With the upper limit from the radio observations we conclude that the IR excess must have another reason. Indeed, the inspection of the IRAS Point Source Catalogue for HD 53138 indicates that the 10 micron flux measured by Barlow & Cohen is peculiarily high compared with the values at lower and higher wavelengths. For all other objects in common with Barlow & Cohen our mass-loss rates do not lead to severe discrepancies with the measured IR excesses, if the accuracy of the photometry is taken into account. (We have also investigated the CDS Catalog of Infrared Observations, Edition 5 by Gezari et al. and realized that for many of our targets the IR-photometry shows a sigificant scatter. We attribute this to the photometric variability of B-supergiants, which makes it difficult to measure an IR-excess unless the spectral energy distribution is observed simultaneously.).

6. Spectral analysis of A-supergiants

The crucial problem for A-supergiants is to find luminous objects in the solar neighbourhood with reasonably determined distances. So far, we have only four objects in our sample and we have to admit that the distance to the brightest object HD 92207 in Car OB1 is quite uncertain. Originally, it was assigned a distance modulus of only $11\overset{m}{.}1$ by Humphreys (1970) although this star was also referenced as a member of the cluster NGC 3324 which is accredited with a distance modulus of $12\overset{m}{.}5$ by Lyngå (1970). Blaha & Humphreys (1989) obtain a distance modulus of $12\overset{m}{.}0$ for Car OB1. The problem with obtaining an accurate distance to this star is that it lies in the direction of the Car OB1 association and the line of sight is along a galactic spiral arm. The distance to the association, and to HD 92207 assuming it is a member, has been discussed quite thoroughly in the literature, most frequently in connection with the distance to the η Car nebula and the very young clusters Tr14 and Tr16. Estimates of these distances range from distance moduli of $12\overset{m}{.}3$ to $12\overset{m}{.}7$ (Walborn 1995, Massey & Johnson 1993), while Shobbrook & Lyngå (1994) summarize the stellar cluster content and extent of Car OB1 (see their Fig. 3) showing that the young star population is distributed in depth over 2 to 3 kpc. We therefore adopt a distance modulus of $12\overset{m}{.}5$ for HD 92207 but acknowledge that there is a large inherent uncertainty in this value.

Photometric data, cluster membership and spectral type for all objects are summarized in Table 4. M_v values are determined in the same way as for the B-supergiants.

Table 4. Spectral types and photometric data of A-supergiants

star	spectral type	assoc.	m_v	B-V	E(B-V)	M_v
HD			mag	mag	mag	mag
92207	A0Ia	Car OB1	5.45	0.50	0.48	-8.54
12953	A1Ia	Per OB1	5.67	0.61	0.59	-7.75
14489	A2Ia	Per OB1	5.17	0.37	0.32	-7.51
223385	A3Ia	Cas OB5	5.43	0.67	0.62	-7.99

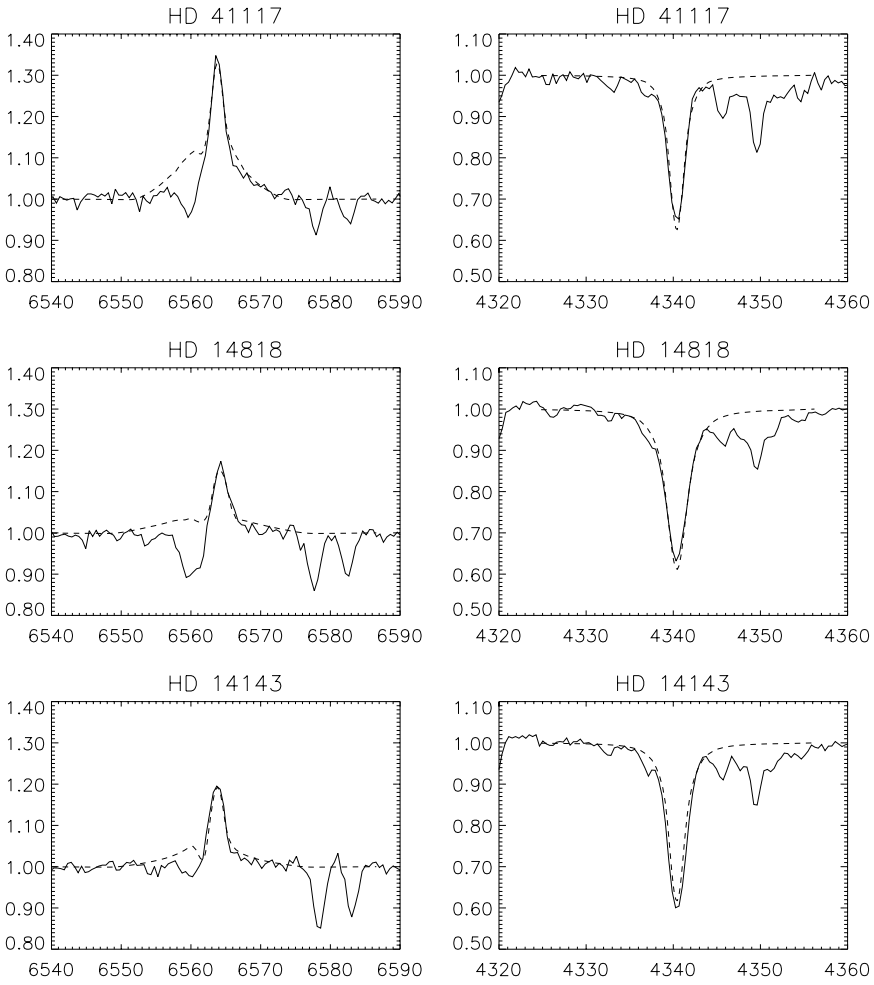

Fig. 3. H_α (left) and H_γ (right) line profile fits of the B2 Ia-supergiants.

6.1. Stellar parameters

As for the B-supergiants, the stellar parameters are obtained from the quantitative analysis of the stellar spectrum. The model atmosphere fit using NLTE line formation calculations on top of metal line blanketed Kurucz atmospheres of the Mg I/II ionization equilibrium and the H_γ profile yields effective temperature and gravity (see Venn 1995b, Przybilla et al. 1999). Then, our unified models, which are unblanketed to reduce the computational effort, are applied to obtain the stellar wind parameters. To compensate for the neglect of blanketing we have used effective temperature values 400 K higher than those obtained with blanketed models in the wind calculations (see also McCarthy et al. 1997). (Table 5 lists the effective temperatures obtained from line blanketed models). The radii are then derived exactly in the same way as for the B-supergiants and also the gravities are iterated taking into account the influence of winds on H_γ. (Table 5 contains the $\log g$ values obtained after this iteration). Normal helium abundance is again adopted for all calculations, except for HD 92207 for which Przybilla et al. (1999), in their recent analysis, found an enhanced helium abundance. We adopt N(He)/N(H)=0.2 for this object.

6.2. Stellar wind properties

In the analysis of the Balmer lines to obtain the stellar wind parameters simultaneously with the gravity we follow exactly the procedure outlined by McCarthy et al. (1997). The strength of the H_α emission peak determines the mass-loss rate $\dot{M}$, when the width of the emission peak is used to constrain β and the blueshift of the absorption yields v_∞. The gravity follows from the wings of H_γ. The stellar wind turbulent velocity v_t is obtained from the redshift of the emission peak with regard to the photospheric radial velocity. As explained in detail by SPH and McCarthy et al. (1997) the inclusion of non-coherent electron scattering in the radiative transfer calculation of the Balmer lines is crucial to obtain a reliable fit. Fig. 6 gives an impression of the quality of the fits obtained.

The results of the analysis are compiled in Table 5. While the terminal velocities of all four objects are very similar, the mass-loss rates vary significantly with luminosity. From Fig. 6 one can learn, how the strengths of the stellar winds influences the Balmer lines of A-supergiants. The H_α profile of HD 14489 – the object with the lowest luminosity and largest gravity – is least affected by stellar wind emission. The profile fits of the Balmer lines are very satisfactory. The general P Cygni shape of H_α and the photospheric absorption wings of H_γ are simulta-

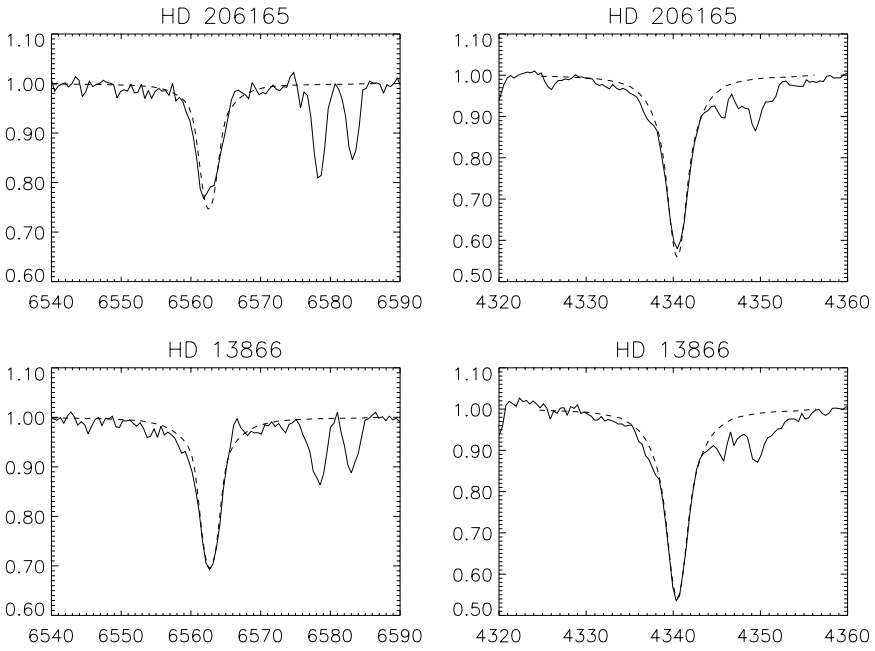

Fig. 4. H_α (left) and H_γ (right) line profile fits of the B2 Ib supergiants.

Table 5. Stellar parameters and stellar wind properties of A-supergiants

star	$T_{\rm eff}$	R_*	$\log g$	$\log L/L_\odot$	$v_{\rm rot}$	$v_{\rm t}$	β	v_∞	$\dot{M}$	$\log D_{\rm mom}$
HD	kK	$R_\odot$	cgs		km s^{-1}	km s^{-1}		km s^{-1}	$10^{-6}M_\odot$/yr	cgs
92207	9.4	192.	0.95	5.41	35	15	1.0	235.	1.31	28.43
12953	9.1	145.	1.10	5.11	35	10	1.5	150.	0.43	27.69
14489	9.0	128.	1.45	4.99	40	20	2.5	190.	0.14	27.27
223385	8.4	174.	0.85	5.13	30	10	1.5	190.	0.65	27.91

neously well reproduced. Small deviations between theory and observation in the line cores are attributed to stellar wind variability (see Kudritzki 1999b) or the imperfectness of the (still) unblanketed model atmospheres. This will require further investigations. The electron scattering wings of HD 12953 and HD 223385 are also represented well by the theory. However, the fit of HD 92207 is somewhat problematic. H_α shows very pronounced electron scattering wings which requires a very low gravity for the fit at this temperature to have sufficient electron scattering optical depth and pathlength in the photosphere. However, then these scattering wings are also weakly present in H_γ causing a slight deviation from the observed profile. This may be a problem of the data reduction in terms of continuum rectification at blue wavelengths but it could also be an indication of the imperfectness of the present model atmosphere approach. (Since the electron scattering wings are formed in the hydrostatic photosphere – see references mentioned above– the discrepancy cannot be attributed to a possible clumpiness in the stellar wind as for objects with very strong mass-loss such as Wolf-Rayet stars). Enhancing the gravity by 0.07 dex (see Fig. 7) improves the H_γ fit significantly but weakens the H_α scattering wings. We conclude that the uncertainties in gravity and mass-loss rate induced by this disturbing inconsistency are small. However, it will be important to investigate its physical background in future work.

The accuracy of the stellar wind parameters obtained by the H_α fits is comparable to McCarthy et al. (1997). Both mass-loss rates and terminal velocities can be fitted within 20 percent accuracy yielding an uncertainty of 0.15 dex for the wind momentum of an individual object. In addition, the determination of v_∞ from H_α might lead to results systematically different from the study of UV lines such as the MgII resonance lines or FeII lines arising from the ground state. So far, there are not enough results published to allow a careful investigation of this question. However, a comparison with Lamers et al. (1995), who used IUE high resolution spectra to determine terminal velocities of blue supergiants, shows acceptable agreement for the three objects in common, HD 92207 (200 ± 30 km s^{-1}), HD 12953 (170 ± 20 km s^{-1}) and HD 14489 (150 ± 20 km s^{-1}).

7. Wind momenta and luminosities

Modified stellar wind momenta

$$D_{\rm mom} = \dot{M} v_\infty (R_*/R_\odot)^{0.5} \quad (3)$$

as function of luminosities are given in Table 3, Table 5 and shown in Fig. 8. To investigate the effects of temperature dependence we have included the O Ia and Ib supergiants from the

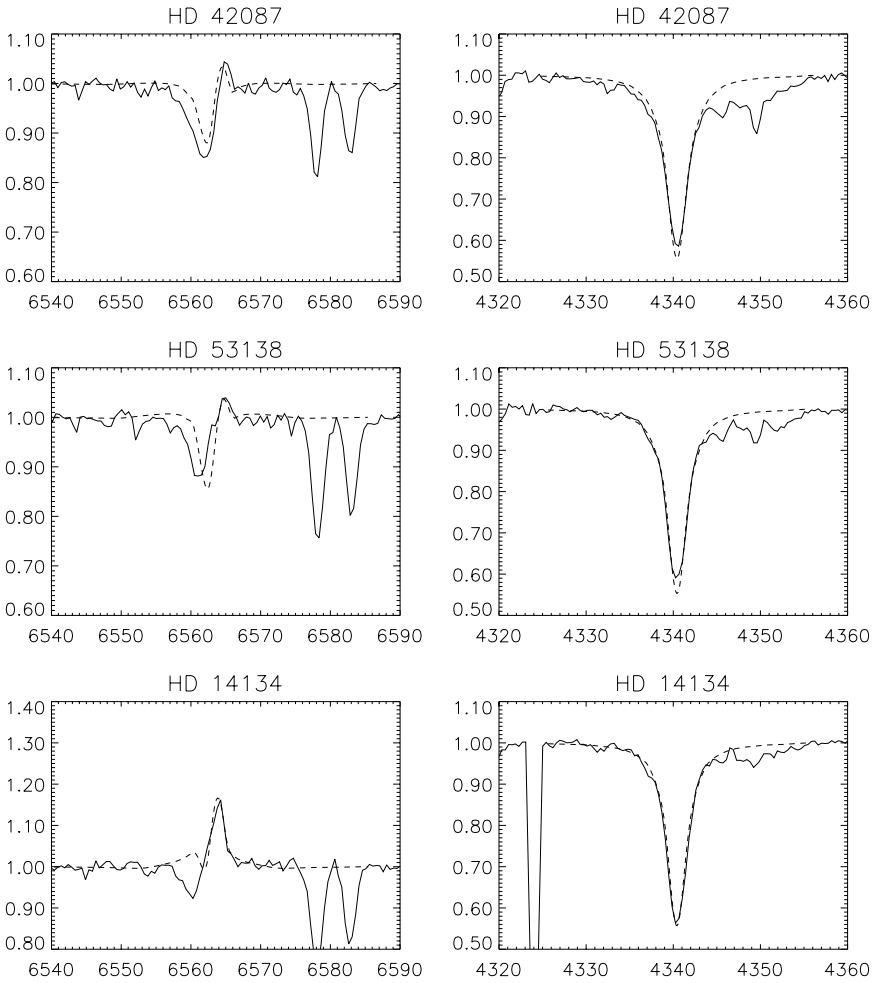

Fig. 5. H_α (left) and H_γ (right) line profile fits of the B2.5- and B3-supergiants.

work by Puls et al. (1996). Fig. 8 reveals several trends. Wind momenta are definitely correlated with the stellar luminosities. However, the wind momentum – luminosity relationship (WLR) shows a distinct dependence on spectral type. Wind momenta are largest for the O-supergiants and then decrease with decreasing effective temperature. The early B spectral types between B0 to B1 have wind momenta about 0.35 dex smaller than the O-supergiants (note that the O-supergiant with the smallest wind momentum in Fig. 8, HD 18409, is of spectral type O9.7 Ib. It is not included in the calculation of the O-supergiant regression curves). The spectral types later than B1 (mid B by our definition) show even weaker winds reduced by roughly 1.1 dex in wind momentum relative to the O-supergiants. A-supergiants, on the other hand, have wind momenta between those of early and mid B spectral types.

Adopting a WLR of the form

$$\log D_{\rm mom} = \log D_0 + x \log(L/L_\odot), \quad (4)$$

we can determine the coefficients log D_0 and x by linear regression (see Fig. 8 and Table 6). The reciprocal value of the slope x may be interpreted as the effective exponent $\alpha_{\rm eff}$ describing the depth dependence of the radiative line force. In the theory of line driven winds $\alpha_{\rm eff}$ can be expressed as the difference of two dimensionless numbers, α and δ, the usual force multiplier parameters of the radiative line force. α corresponds to the power law exponent of the line strengths distribution function controlling the relative contribution of strong and weak lines to the radiatiative acceleration, whereas δ describes the depth variation induced by ionization changes of the total number of lines contributing (see Abbott 1982, Kudritzki et al. 1989, Puls et al. 1996, Kudritzki 1998, Kudritzki et al. 1998, Puls et al. 1999 for a more detailed discussion). Typical values for O-stars are α = 0.7 to 0.6 and δ = 0.1 to 0.0,

$$\alpha_{\rm eff} = 1/x = \alpha - \delta. \quad (5)$$

Changes in the slope x of the WLR as function of spectral type are therefore an additional indication that the winds are driven by different sets of ions. From Table 6 (see also Fig. 8) we infer

Table 6. Coefficients of the wind momentum – luminosity relationship for A-, B- and O-supergiants of the solar neighbourhood.

sp. type	log D_0	x	$\alpha_{\rm eff}$
A	14.22±2.41	2.64±0.47	0.38±0.07
mid B	17.07±1.05	1.95±0.20	0.51±0.05
early B	21.24±1.38	1.34±0.25	0.75±0.15
O	20.40±0.85	1.55±0.15	0.65±0.06

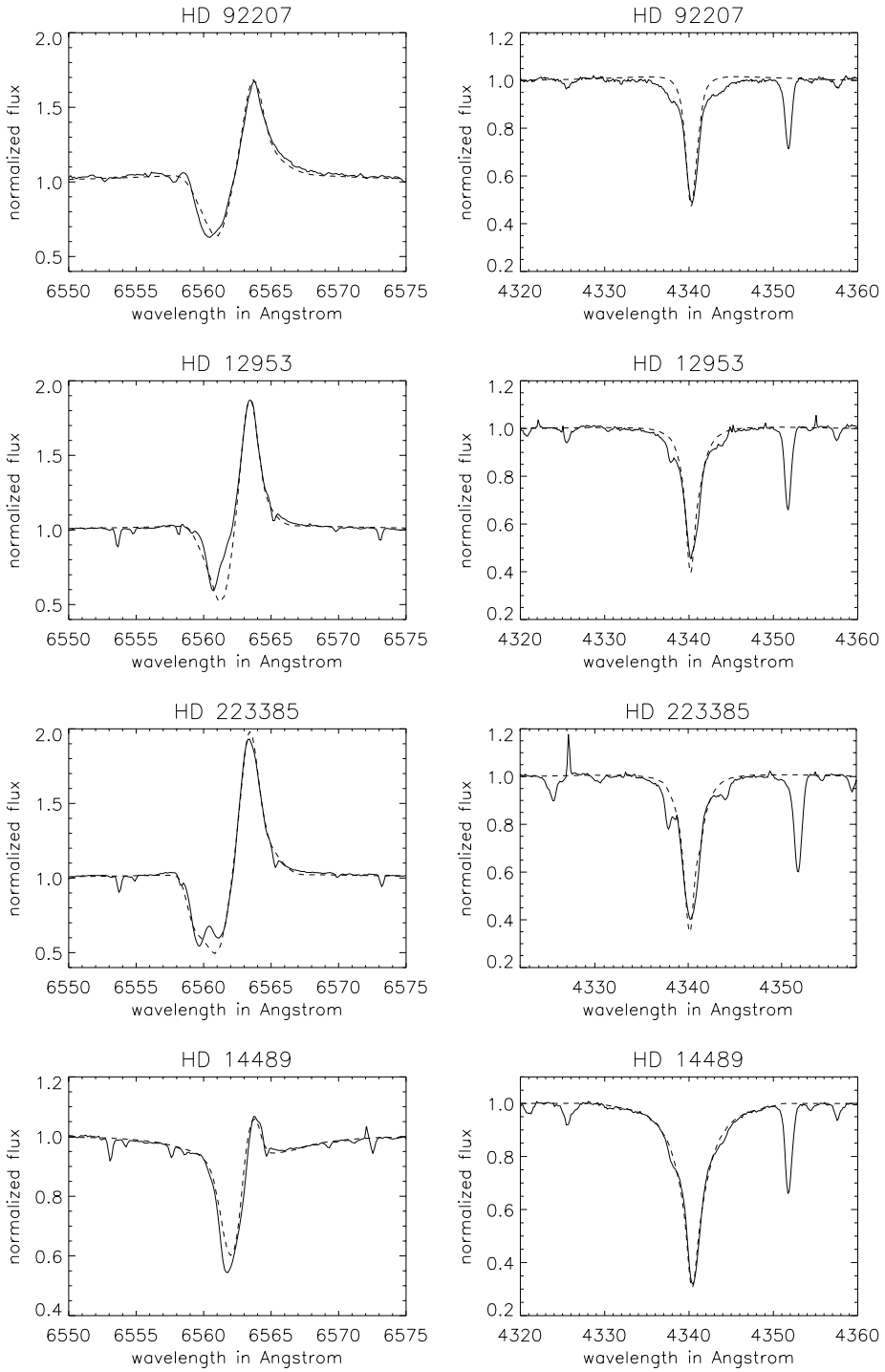

Fig. 6. H_α (left) and H_γ (right) line profile fits of the galactic A-supergiants.

that the WLR is definitely steeper for the spectral types mid B and A than for O-supergiants (although the value for the A-supergiants is uncertain because of the small number of objects). This is exactly what one expects, if spectral lines of the iron group at lower ionization stages (III and II) absorb the photon momentum and drive the wind (Puls et al. 1999). The slope of the early B WLR depends on the uncertain distance of the low luminosity object HD 38771 and would become steeper, if the Hipparcos parallax is too large because of the effects of the Lutz-Kelker bias (see Reid 1998). Therefore, the difference to the O-supergiants in Table 6 is very likely not significant.

The variation of height D_0 of the WLR is a more complex matter, since this quantity depends on the *flux weighted* total number of spectral lines as well as on $\alpha_{\rm eff}$ and α itself (Puls et al. 1999). Only in cases of similar slopes a comparison of D_0 gives direct insight into the *absolute* number of effectively driving lines, whereas in all other cases their *distribution* with

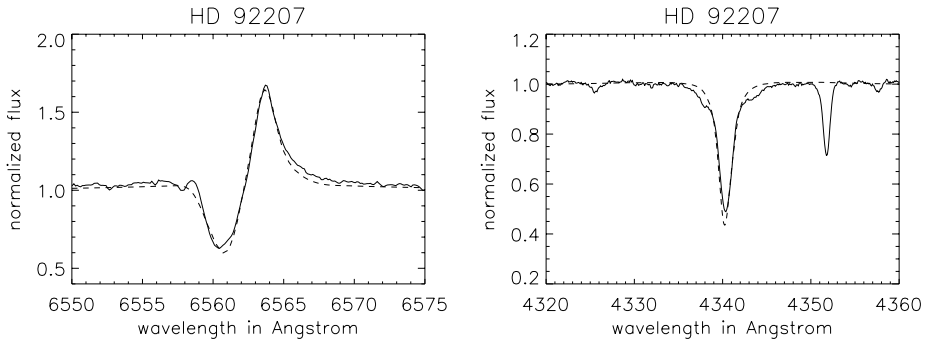

Fig. 7. H_α and H_γ fits of HD 92207 for the same parameters as in Table 5 but $\log g$ = 1.00 and $\dot{M} = 1.6\ 10^{-6} M_\odot$/yr.

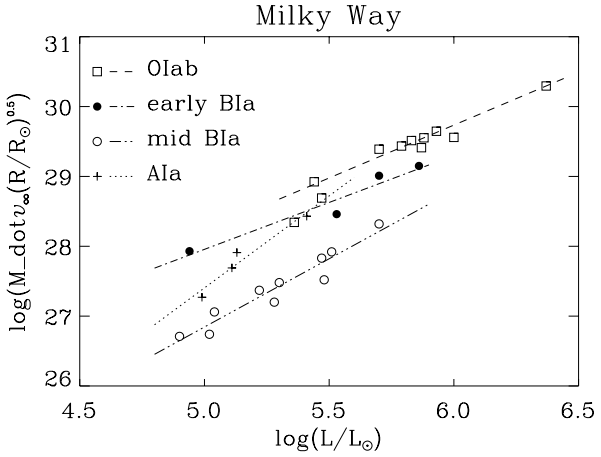

Fig. 8. Wind momenta as function of luminosities for galactic supergiants of spectral types O, B (early B: B0 to B1; mid B: B1.5 to B3) and A. The straight lines for each group of spectral types are the corresponding regression curves.

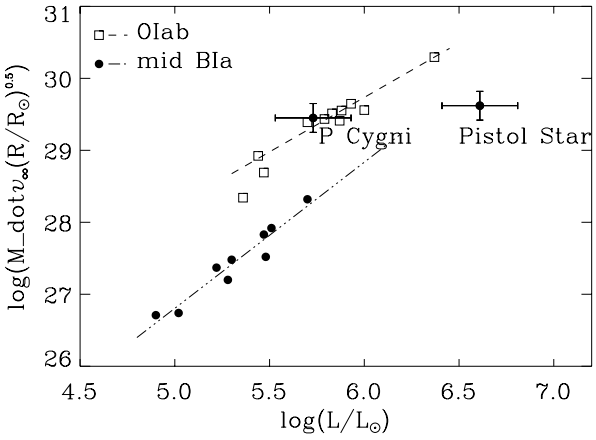

Fig. 9. Wind momentum as function of luminosity for galactic supergiants of spectral type O and mid B compared with the wind momentum of the very luminous Pistol Star in the Galactic Centre and the extreme Luminous Blue Variable P Cygni.

respect to line-strength (α) has a significant influence on the offset.

Due to its (partial) dependence on flux-weighted line number, D_0 varies between spectral types not only because of ionization changes but also because of the different spectral locations of the lines with regard to the flux maximum and absorption edges such as the hydrogen Lyman- and Balmer-edges. At least with respect to the observed differences in D_0 between O-type and A-type supergiants (accounting for the changes in $\alpha_{\rm eff}$), this interpretation seems to be correct, as demonstrated by Puls et al. (1999). However, to predict the variation of D_0 over the whole range of effective temperatures and thus to check whether our present interpretation is generally valid will require more detailed calculations of radiation driven wind models in the future. We feel that especially the pronounced drop in D_0 between effective temperatures of 23500 K and 22500 K (on our temperature scale of unblanketed models) will provide a challenge for the theory. A detailed spectroscopic study of a larger sample of objects in this transition range of temperatures to disentagle stellar wind properties in more detail will certainly be extremely valuable. In addition, a careful re-investigation whether systematic effects (for instance, deviations of the helium abundances from the normal value or metal line blanketing and blocking in this temperature range) may have influenced the results of the spectroscopic analysis will be important.

The observed WLR of "normal" supergiants of mid B spectral type allows a comparison with more extreme objects of comparable spectral type. Very recently, Figer et al. (1998) have investigated the physical properties of the spectacular "Pistol Star" in the Galactic Centre. In their detailed spectroscopic study using high quality IR spectra and unified NLTE model atmospheres with winds they have found that this object has a luminosity of $\log L/L_\odot$ = 6.6 and is one of the most luminous and – therefore – most massive stars known so far. However, despite of the extreme luminosity the stellar wind of this object is surprisingly weak. Figer et al. (1998) obtain $\dot{M} = 3.8\ 10^{-5} M_\odot$/yr, $v_\infty = 95$ km s^{-1} and $\log D_{\rm mom} = 29.62$ for mass-loss rate, terminal velocity and modified wind momentum, respectively. This is roughly 1.0 dex less than one would expect for an O-star of the same luminosity. Ignoring the spectral type dependence of the WLR one would be tempted to conclude that the Pistol Star is probably an unresolved multiple system of less luminous objects, although the careful investigation by Figer et al. (1998) does not give any indication in this direction. However, the effective temperature obtained for this object in their NLTE analysis is $T_{\rm eff}$ = 14100 K and it is, therefore, more appropriate to compare with the our new WLR of mid B spectral types. This

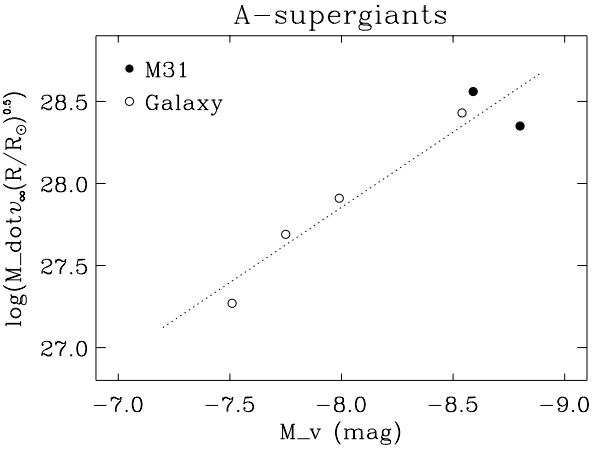

Fig. 10. Wind momentum of galactic and M31 A-supergiants as function of absolute visual magnitude. The data of the M31 objects are from McCarthy et al. (1997). The dashed curve is the linear regression obtained from all objects.

is done in Fig. 9. Given the uncertainties of the complex analysis of the Galactic Centre IR-data and the fact that the Pistol Star is somewhat cooler than B3 Ia-supergiants, we conclude from a comparison of wind momenta that this object may indeed be a single object of extreme luminosity but with a "normal" stellar wind.

On the other hand, we note from Figer et al. (1998) that the Pistol Star is located in a "sparsely populated zone in the HRD beyond the Humphreys-Davidson-limit where unstable stars of the Luminous Blue Variable type are found". It is quite surprising that such a star exhibits just a normal stellar wind. This becomes more evident, if we add the proto-type Luminous Blue Variable P Cygni to Fig. 9. This object has been studied by Lamers et al. (1996) and Najarro et al. (1997) (see also Pauldrach & Puls 1990, Langer et al. 1994) and has an effective temperature of $T_{\rm eff}$ = 18100 K corresponding to our specral types B2 and B3. With $\log L/\mathrm{L}_\odot$ = 5.75 its luminosity is only slightly higher than the one of HD 41117 the most luminous "normal" mid B-supergiant in our sample. However, with $\dot{M} = 3.0\ 10^{-5}\mathrm{M}_\odot$/yr, $v_\infty = 185\,\mathrm{km\,s^{-1}}$ and $\log D_{\rm mom} = 29.48$ the wind momentum of P Cygni is 1.2 dex larger than expected from our regression relation for this spectral type.

The explanation for this behaviour has already been worked out by Lamers et al. (1995) in their discussion of the "bi-stability of B-supergiant winds". P Cygni is very likely an object that has undergone substantial mass-loss in its evolutionary history and is therefore rather close to the Eddington limit (see Langer et al. 1994). It is definitely helium enriched and the rather small terminal velocity leads to the conclusion that the gravity (and therefore the mass) must be very small. Langer et al. (1994) estimate $\log g$ = 2.0 from their wind models which are also able to reproduce the observed high wind momentum. Our "normal" objects have significantly higher gravities and are more distant from the Eddington limit. However, as Pauldrach & Puls (1990) and Lamers & Pauldrach (1991) have shown for the temperature range of B1.5 to B3 supergiants, the distance to the Eddington limit – below a critical threshold – is crucial for the strengths of stellar winds. Closer to the Eddington limit the radiation driven wind becomes slower and denser which increases the stellar wind optical thickness in the Lyman continuum and – in the temperature range between B1.5 and B3 spectral types – suddenly affects the ionization of iron group elements, which can lead to a strong increase of stellar wind momentum. We therefore assume that the difference in gravity (or stellar mass) is the reason for the difference between the "normal" supergiants and the extreme object P Cygni. In this sense, the pistol star must either be a "normal" object sufficiently away from the Eddington limit or the reduced flux in the Lyman continuum at $T_{\rm eff}$ = 14000 K (relative to 22000 to 18000 K) leads to a more moderate stellar wind. Of course, this whole scenario will have to be confirmed by a comprehensive calculation of stellar wind models in the appropriate range of stellar parameters.

8. Stellar wind momenta and extragalactic distances

It has long been a dream of stellar astronomers to use the most luminous blue stars as individuals to determine the distances to other galaxies. Evidently, the existence of the WLR provides a unique opportunity to obtain information about absolute magnitudes from a purely spectroscopic analysis of the stellar wind lines. To illustrate the situation we show the modified wind momenta of our A-supergiants as function of absolute visual magnitude in Fig. 10. We have included the two A-supergiants in M31 studied recently by McCarthy et al. (1997) in their analysis of Keck HIRES spectra. The diagram is exciting for several reasons. It demonstrates that the galactic objects agree well with objects in another galaxy to form a nice WLR with only a small scatter around the mean relationship (the fact that the use of absolute magnitude on the abscissa instead of luminosity leads to a similarily well defined relationship reflects only that the bolometric corrections are small). In addition, the relationship holds to absolute magnitudes up to $\mathrm{M_v} = -9^{\rm m}$, i.e., objects of tremendous intrinsic brightness easily to detect and to investigate spectroscopically in distant galaxies.

However, for the use of the WLR as a distance indicator Fig. 10 is somewhat misleading, since the determination of a mass-loss rate from an H_α profile requires already the a priori assumption about the stellar radius and therefore the distance. Changing the distance d or the distance modulus μ of an object in Fig. 10 by

$$d_{\rm new} = \alpha d_{\rm old} \tag{6}$$

$$\Delta\mu = 5\log\alpha \tag{7}$$

results in a shift of the ordinate by

$$\Delta \log D_{\rm mom} = 2\log\alpha \tag{8}$$

since one can show analytically (Puls et al. 1996) that the quantity

$$Q = \dot{M}(R_*/R_\odot)^{-1.5} \tag{9}$$

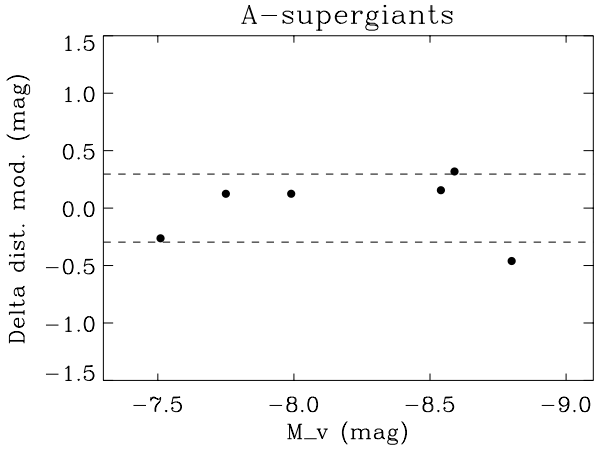

Fig. 11. Residua in distance modulus $\Delta\mu$ obtained for the A-supergiants of Fig. 10 (see text). The dashed curves indicate the standard deviation $\sigma_{\rm A} = 0\overset{\rm m}{.}30$.

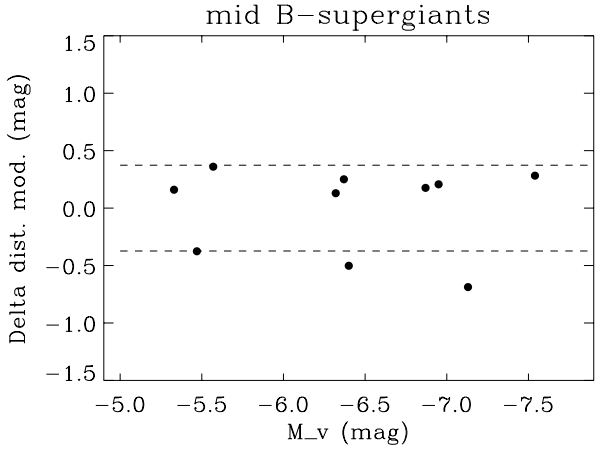

Fig. 12. Residua in distance modulus $\Delta\mu$ obtained for the mid B-supergiants of Fig. 8 (see text). The dashed curves indicate the standard deviation $\sigma_{\rm B} = 0\overset{\rm m}{.}37$.

is an invariant of the profile fitting process, i.e. the strength of H_α as a stellar wind line scales exactly with this quantity. For instance, assuming a larger distance (and therefore radius) for an observed object one would have to increase $\dot{M}$ so that Q remains constant to obtain a similar fit of the H_α profile.

The above equations allow to use the scatter around the regression curve of Fig. 10 for an estimate of the accuracy in distance modulus μ which can be obtained. With the regression fit

$$\log D_{\rm mom} = a_{\rm A} + b_{\rm A} M_{\rm v} \tag{10}$$

($a_{\rm A} = 20.52, b_{\rm A} = -0.916$) we can calculate residuals ϵ_i from the regression for each individual object i

$$\epsilon^i_{\rm A} = \log D^i_{\rm mom} - a_{\rm A} - b_{\rm A} M^i_{\rm v} \tag{11}$$

A change in distance modulus of (see Eqs. 7,8,9)

$$\Delta\mu_i = 5 \log \alpha_i = -\epsilon^i_{\rm A}/(0.4 + b_{\rm A}) \tag{12}$$

would shift each object i exactly on the regression. Hence, these values of $\Delta\mu_i$ can be used as an estimate of the accuracy in distance modulus (see Fig. 11). The standard deviation obtained from these residua is $\sigma_{\rm A} = 0\overset{\rm m}{.}30$.

We can apply a similar procedure for the mid B-supergiants. Since bolometric corrections are larger than for A-supergiants, we use the original WLR with $\log L/{\rm L}_\odot$ on the abscissa and ($a_{\rm B} = 17.07$, $b_{\rm B} = 1.95$)

$$\log D_{\rm mom} = a_{\rm B} + b_{\rm B} \log L/{\rm L}_\odot \tag{13}$$

$$\epsilon^i_{\rm B} = \log D^i_{\rm mom} - a_{\rm B} - b_{\rm B} \log L^i/{\rm L}_\odot \tag{14}$$

$$\Delta\mu_i = 5 \log \alpha_i = 2.5\epsilon^i_{\rm b}/(b_{\rm B} - 1). \tag{15}$$

The corresponding residua $\Delta\mu_i$ are shown in Fig. 12. The standard deviation is $\sigma_{\rm B} = 0\overset{\rm m}{.}37$.

This confirms the estimate by McCarthy et al. (1997) that with ten to twenty objects per galaxy, distance moduli as accurate as $0\overset{\rm m}{.}1$ should be achievable. The idea is to carry out multi-object spectroscopy with 8m-class telescopes combined with HST photometry to obtain stellar parameters ($T_{\rm eff}$, $\log g$, abundances) and reddening in a first step. Then determination of Q from H_α (for A-supergiants one would also obtain v_∞ from H_α) and the application of a properly calibrated WLR would yield the absolute magnitude. Comparison with the dereddened apparent magnitude would, finally, allow to determine the distance.

The uncertainties in WLR distance moduli appear to be comparable to those obtainable from Cepheids in galaxies. The advantage of the WLR-method, however, is that individual reddening (and therefore extinction) as well as metallicity (see discussion below) can be derived directly from the spectrum of every object. Moreover, it is a new independent primary method for distance determination and can contribute to the investigation of systematic errors of extragalactic distances. However, the crucial question is out to which distances will the method be applicable.

The best spectroscopic targets at large distances are certainly A-supergiants such as shown in Fig. 10. Since massive stars evolve at almost constant luminosity towards the red, A-supergiants are the optically brightest "normal" stellar objects because of the effects of Wien's law on the bolometric correction. In addition, we can determine the wind momenta of these objects solely by optical spectroscopy at H_α (without need of the UV). This means that we can use ground-based telescopes of the 8m class for spectroscopy rather than the "tiny" HST (which is then needed for accurate photometry only).

From Fig. 10 we see that the brightest A-supergiants have absolute magnitudes between -9$^{\rm m}$ and -8$^{\rm m}$. Such objects would be of apparent magnitude between $20^{\rm m}$ and $21^{\rm m}$ in galaxies 6 Mpc away, certainly not a problem for medium (2 Å) resolution spectroscopy with 8 m class telescopes. Even in a galaxy like M100 at a distance of 16 Mpc (Freedman et al. 1994b; Ferrarese et al. 1996) these objects would still be accessible at magnitudes around $22\overset{\rm m}{.}5$ and would yield wind momentum distances. Indeed, the HST colour magnitude diagram published by

Freedman et al. (1994a) may show the presence of such objects in M100.

One might ask, of course, whether a medium resolution of 2 Å would still allow a sufficiently accurate determination of effective temperature, surface gravity, abundances, and wind momentum. We note that the rotational velocities of A-supergiants are typically on the order of $40\,\mathrm{km\,s^{-1}}$, a broadening which is matched by a spectral resolution of roughly 1.4 Å at H_α. Therefore we expect that the medium resolution situation will not be dramatically worse, provided sufficient S/N can be achieved and accurate sky-, galaxy-, and HII region background subtraction can be performed at very faint magnitudes. Experiments with observed spectra degraded with regard to S/N, resolution and sky emission indicate that such observations are challenging but feasible.

9. Future work

In summary of the previous sections it is certainly fair to conclude that the concept of the spectral dependend WLR appears to be an excellent tool to discuss the strengths of stellar winds and to use the most luminous "normal" blue supergiants as extragalactic distance indicators. However, it became also clear that what has been presented here can only be regarded as a first step. Investigations in many directions will be neccessary to establish the WLR-concept reliably. In the following we discuss the most important next steps.

Galactic calibration. So far the galactic WLR-calibration is based only on a small number of objects with reliable distances per spectral type group. The numbers are particularily small for early B-supergiants and A-supergiants. In the near future before the next astrometric space projects become reality, the only possibility to improve the situation is the careful re-investigation of existing catalogues with regard to cluster and association membership and improved reddening corrections. In addition, one might use the progress obtained with alternative distance indicators such as eclipsing binaries (Clausen 1999), Cepheids using the IR-Baade-Wesselink-Method (Gieren 1999) etc. to use Local Group galaxies like M31 and M33 as additional calibrators.

Spectral Variability. It is well known that H_α-profiles of A- and B-supergiants vary as a function of time (see, for instance, Kaufer et al. 1996). This does, of course, mean that wind momenta derived in the way as described above will also vary and, therefore, affect the WLR. Very recently, Kudritzki (1999b) has discussed the problem for the case of the A-supergiant HD 92207 and found that the uncertainty in wind momentum introduced by the spectral variability of this object is smaller than 0.15 dex. He concluded that part of the intrinsic scatter of the WLR might be caused by variability but that the concept of the WLR is not affected by uncertainties of this magnitude, in particular, if many objects are investigated per galaxy. However, so far this conclusion is based on the investigation of one object only. Many others studies will have to be carried out as function of spectral type and luminosity class to confirm or to disprove this conclusion.

Metallicity Dependence. Since the winds of blue supergiants are driven by absorption of photon momentum through metal lines, stellar wind momenta must depend on metallicity in a sense that wind momenta become weaker with decreasing metallicity. For normal O-stars, this metallicity dependence has been discussed carefully by Abbott (1982), Kudritzki et al. 1987, Puls et al. (1996 and 1999). Observations of O-stars in the Magellanic Clouds with HST have led to a general confirmation of the theory (see Puls et al. 1996). However, for supergiants of spectral type A and mid B only little work has been done so far. Observing two A-supergiants in M33 with Keck and HIRES and making use of the strong metallicity gradient in this galaxy, McCarthy et al. (1995) were able to demonstrate that drastic metallicity effects are encountered, if the metallicity drops below the SMC value. In addition, a few B-supergiants have been studied in the Magellanic Clouds (Kudritzki 1998). However, a systematic survey in the Magellanic Clouds, NGC 6822, M31 and M33 is now under way by the authors of this paper and their collaborators to close this gap and to provide an empirical calibration of WLR metallicity dependence. In addition, theoretical work will be carried out for these spectral types as well.

Wind momenta beyond the Local Group. This is the final goal of the project. As discussed above, quantitative spectroscopy of blue supergiants beyond the Local Group to determine the strengths of stellar winds and wind momenta is feasible with 8m-class telescopes and medium resolution spectrographs. Whether or not this will lead to a new, independent determination of extragalactic distances is open until the prove is made by the appropriate analysis of the first set of spectroscopic multi-object observations in a galaxy clearly beyond the Local Group. These observations will become available soon.

Acknowledgements. RPK likes to thank the director and staff of Steward Observatory, Tucson, for their hospitality and support during a sabbatical where much of the stellar wind analysis has been carried out. He also wishes to thank Norbert Przybilla and Oliver Knörndel for discussion and support. The funding through the "Verbundforschung Astronomie" by the Bundesminister für Forschung und Bildung and the DLR under grant 50 R93040 is gratefully acknowledged (DJL, JR). The constructive remarks of the referee, Dr. Paul Crowther, have helped to improve the paper and are very much acknowledged.

References

Abbott D.C., 1982, ApJ 259, 282
Barlow M.J., Cohen M., 1977 ApJ 213, 737
Blaha C., Humpreys R.M., 1989, AJ 98, 1598
Cardelli J.A., Clayton G.C., Mathis J.S., 1989, ApJ 345, 245
Castor J.I., Abbott D.C., Klein R.I., 1975, ApJ 195, 157
Clausen V., 1999, In: Bergeron J., et al., (eds.) Proc. VLT Opening Symposium, Science in the VLT Era and Beyond. in press
Drake S.A., Linsky J.L., 1989, AJ 98, 1831
Ferrarese L., Freedman W.L., Hill R.J., et al., 1996, ApJ 464, 568

Figer D.F., Najarro F., Morris M., et al., 1998, ApJ 506, 384
Freedman W.L., Madore B.F., Stetson P.B., et al., 1994a, ApJ 435, L31
Freedman W.L., Madore B.F., Mould J.R., et al., 1994b, Nat 371, 757
Gabler R., Gabler A., Kudritzki R.P., et al., 1989, A&A 226, 162
Garmany C.D., Stencel R.E., 1992, A&AS 94, 211
Gieren W., 1999, In: Bergeron J., et al. (eds.) Proc. VLT Opening Symposium, Science in the VLT Era and Beyond. in press
Haser S.M., 1995, Ph.D. Thesis, University of Munich
Haser S.M., Lennon D.J., Kudritzki R.P., et al., 1995, A&A 295, 136
Haser S.M., Pauldrach A.W.A., Lennon D.J., et al., 1998, A&A 330, 285
Howarth I.D., Siebert K.W., Hussain G.A., et al., 1997, MNRAS 284, 265
Humphreys R.M., 1970, AJ 75, 602
Kaufer A., Stahl O., Wolf B., et al., 1996, A&A 305, 887
Kudritzki R.P., 1980, A&A 85, 174
Kudritzki R.P., 1998, In: Aparicio A., Herrero A., Sánchez F. (eds.) V III Canary Islands Winter School of Astrophysics on Stellar Astrophysics for the Local Group. Cambridge University Press, 149
Kudritzki R.P., 1999a, In: Livio M. (ed.) Proc. of STScI May 1998 Symposium, Unsolved Problems of Stellar Evolution. in press
Kudritzki R.P., 1999b, In: Wolf B., Stahl O., Fullerton A.W. (eds.) Proc. IAU Coll. No. 169, Springer Verlag, 405
Kudritzki R.P., Pauldrach A.W.A., Puls J., 1987, A&A 173, 293
Kudritzki R.P., Pauldrach A.W.A., Puls J., et al., 1989, A&A 219, 205
Kudritzki R.P., Lennon D.J., Puls J., 1995, In: Walsh J.R., Danziger I.J. (eds.) Proc. of ESO Workshop Science with the VLT. Springer Verlag, 246
Kudritzki R.P., Mendez R.H., McCarthy J.K., et al., 1997, In: Lamers H.J.G.L.M., Habing H.J. (eds.) Proc. IAU Symp. 180, Planetary Nebulae. Kluwer Academic Publishers, 64
Kudritzki R.P., Springmann U., Puls J., et al., 1998, ASP Conf. Series 131, 299
Lamers H.J.G.L.M., Pauldrach A., 1991, A&A 244, L5
Lamers H.J.G.L.M., Snow T.P., Lindholm D., 1995, ApJ 455, 269
Lamers H.J.G.L.M., Najarro F., Kudritzki R.P., et al., 1996, A&A 315, L229
Langer N., Hamann W.R., Lennon M., et al., 1994, A&A 290, 819
Lennon D.J., Dufton P.L., Fitzsimmons A., 1992, A&AS 94, 569
Lennon D.J., Dufton P.L., Fitzsimmons A., 1993, A&AS 97, 559
Lyngå G., 1970, A&A 8, 41
Massey P., Johnson J., 1993, AJ 105, 980
McCarthy J.K., Lennon D.J., Venn K.A., et al., 1995, ApJ 455, L35
McCarthy J.K., Kudritzki R.P., Lennon D.J., et al., 1997, ApJ 482, 757
McErlean N.D., Lennon D.J., Dufton P.L., 1998, A&A 329, 613
McErlean N.D., Lennon D.J., Dufton P.L., 1999, A&A, in press
Najarro F., Hillier D.J., Stahl O., 1997, A&A 326, 1117
Narayanan V.K., Gould A., 1999, ApJ 515, 256
Pauldrach A., Puls J., 1990, A&A 237, 409
Pauldrach A.W.A., Puls J., Kudritzki R.P., 1986, A&A 164, 86
Przybilla N., Butler K., Becker S., et al., 1999, In: Proc. ESO Workshop on Chemical Evolution from Zero to High Redshift. Springer Verlag, in press
Puls J., Kudritzki R.P., Herrero A., et al., 1996, A&A 305, 171
Puls J., Springmann U., Lennon M., 1999, A&AS, in press
Reid N., 1998, AJ 115, 204
Santolaya–Rey A.E., Puls J., Herrero A., 1997, A&A 488, 512
Scuderi S., Panagia N., Stanghellini C., et al., 1998, A&A 332, 251
Shobbrook R.R., Lyngå G., 1994, MNRAS 269, 857
Smith K.C., Howarth I.D., 1998, MNRAS 299, 1146
Venn K.A., 1995a, ApJS 99, 659
Venn K.A., 1995b, ApJ 449, 839
Walborn N.R., 1995, Rev. Mex. Astron. Astrofís. 2, 51